Bulletin of the Earthquake
Research Institute
Vol. 46 (1968), pp. 607-630

26. Crustal Structure in the Profile across the Northeastern Part of Honshu, Japan, as Derived from Explosion Seismic Observations. Part 2. Crustal Structure.

By Michio Hashizume*, Kazuo Oike*, Shuzo Asano**, Hiroyuki Hamaguchi***, Atusi Okada**, Sadanori Murauchi+, Etsuzo Shima** and Mitsuo Nogoshi++

(Read July 18, 1967.—Received Jan. 31, 1968.)

Abstract

The crustal structure in a profile crossing the northeastern part of Honshu, Japan, is derived from the data obtained in the Off Kesennuma, the Off Oga Peninsula and the Tutihata explosions. The fixed array-moving shot point technique was first applied in this profile, and more than 600 seismograms were obtained. Assuming a homogeneous layered structure, the thickness of the crust in the central mountain area was obtained as 30 km. The crust tapers near the shore toward the ocean on both sides of Honshu and the transition of crustal structure from the continental to the oceanic seems to occur in the vicinity of Honshu. The existence of the basaltic layer and the value of 8.0 km/s for Pn velocity became more convincing through the analysis of this profile.

1. Introduction

This paper presents the crustal structure in a profile crossing the northeastern part of Honshu, Japan, derived from the data given in Part 1 under the same title[1]. This profile covers the land area from Kesennuma Bay to Oga Peninsula. Its length at sea is about 130 km

* Disaster Prevention Research Institute, Kyoto University;
** Earthquake Research Institute, University of Tokyo;
*** Geophysical Institute, Tohoku University;
+ National Science Museum;
++ Akita University.

1) The Research Group for Explosion Seismology, *Bull. Earthq. Res. Inst.*, **46** (1968), 529-605.

Table 1.

	Number of explosions	Number of observation sites
Off Kesennuma	20	15
Receiving vessel	60	1
Off Oga Peninsula	21	14
Tutihata	1	14
Total	102	44

on both sides of Honshu. The fixed array-moving shot point technique was applied for the first time in Japan, and the number of data obtained by recent experiments surpassed that in the past[2]. It was a question whether this method could give good results or not since the profile includes a complicated geological area such as the island (Honshu) and its marginal ocean. However, the results obtained are fairly satisfactory, so that the fixed array-moving shot point method is found to be very useful even in the complicated area. The summary of the experiments is given in Table 1, and the number of available seismograms was about six hundred.

2. Travel time analysis

The fundamental procedures and assumptions are as follows:

1) A homogeneous layered structure is assumed. Also it is assumed that there are no faults on each interface.

2) The readings of first and later arrivals are divided into four grades depending upon the clearness of these phases (Part 1). But mainly the first arrivals are used in the following analysis and some of the later arrivals are used as supplementary.

3) A certain amount of discrepancy between observed and calculated travel times, 0.2 sec at ordinary sites, is assumed to be probable because of variations in the thickness and the velocity of surface layer on land and at the sea bottom, the heterogeneity of wave velocity within the crust and in water, the accuracy of shot point determination, the assumption adopted, etc.

2) The RESEARCH GROUP FOR EXPLOSION SEISMOLOGY, *Bull. Earthq. Res. Inst.*, **29** (1951), 27; **30** (1952), 279; **31** (1953), 281; **32** (1954), 79; **33** (1955), 699; **37** (1959), 89, 495.

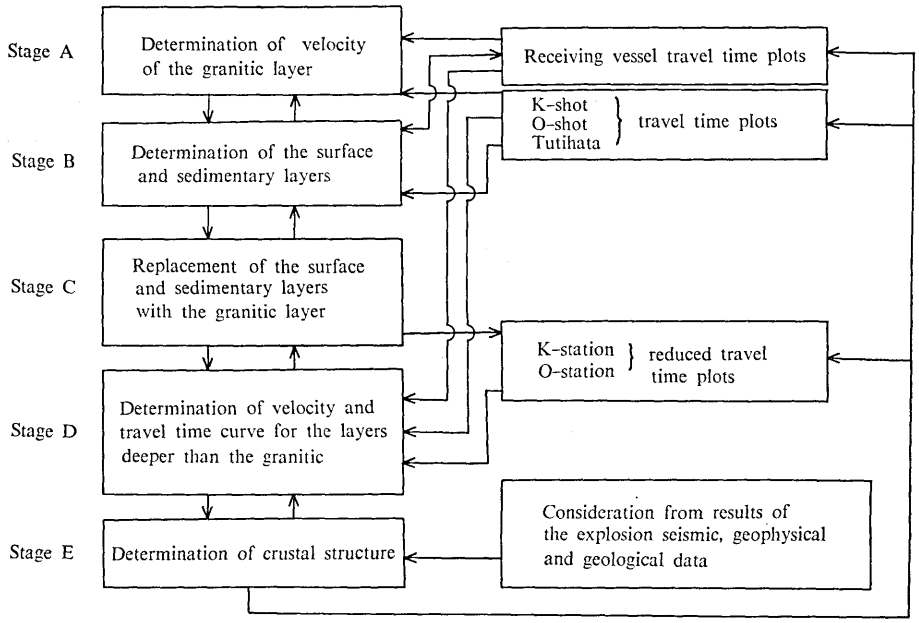

Fig. 1. Flow diagram of the procedures.

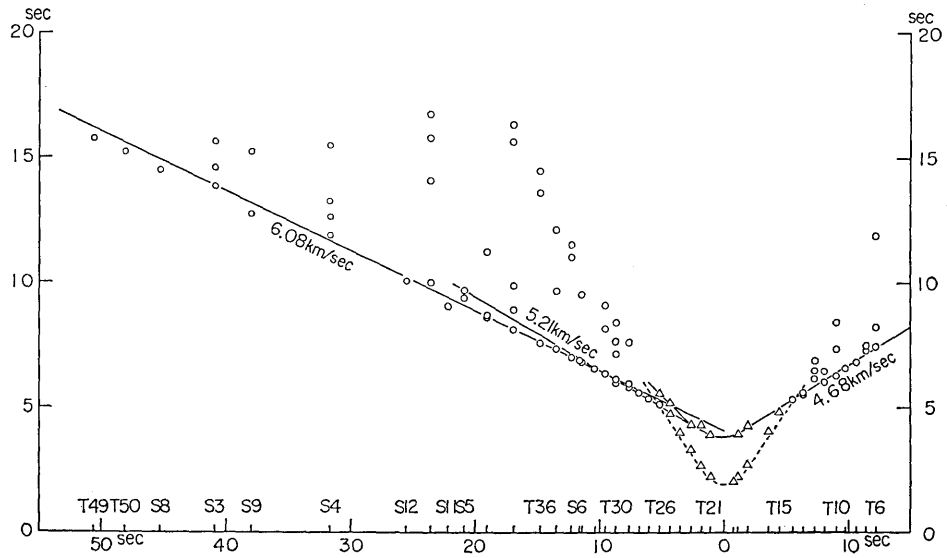

Fig. 2. Travel time plot derived from observations of the receiving vessel, Seihu-maru.

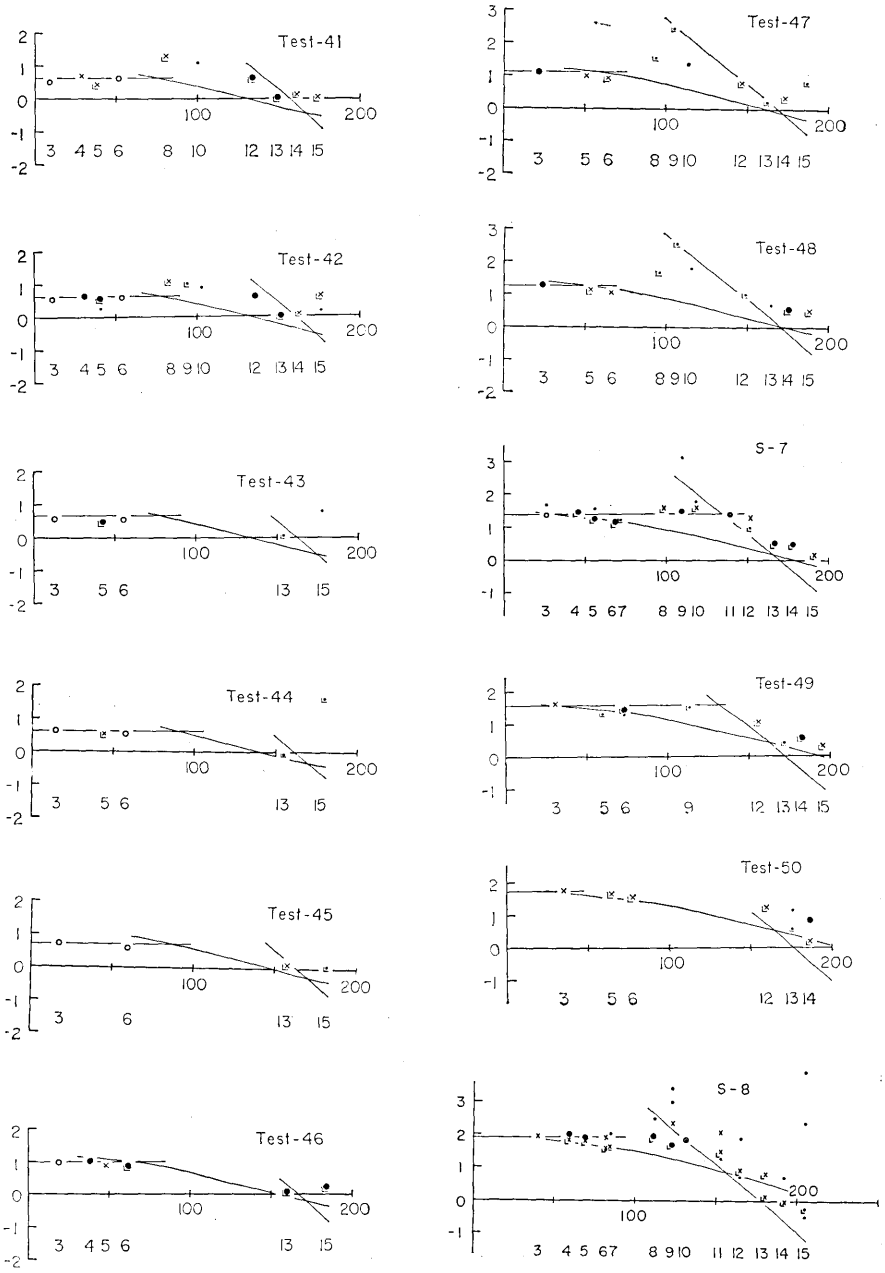

Fig. 3. Reduced travel time plot for each shot in the Off Kesennuma explosions.
abscissa : epicentral distance Δ in km.
ordinate : reduced travel time (T-Δ/6) in sec.
⊙ : class A reading

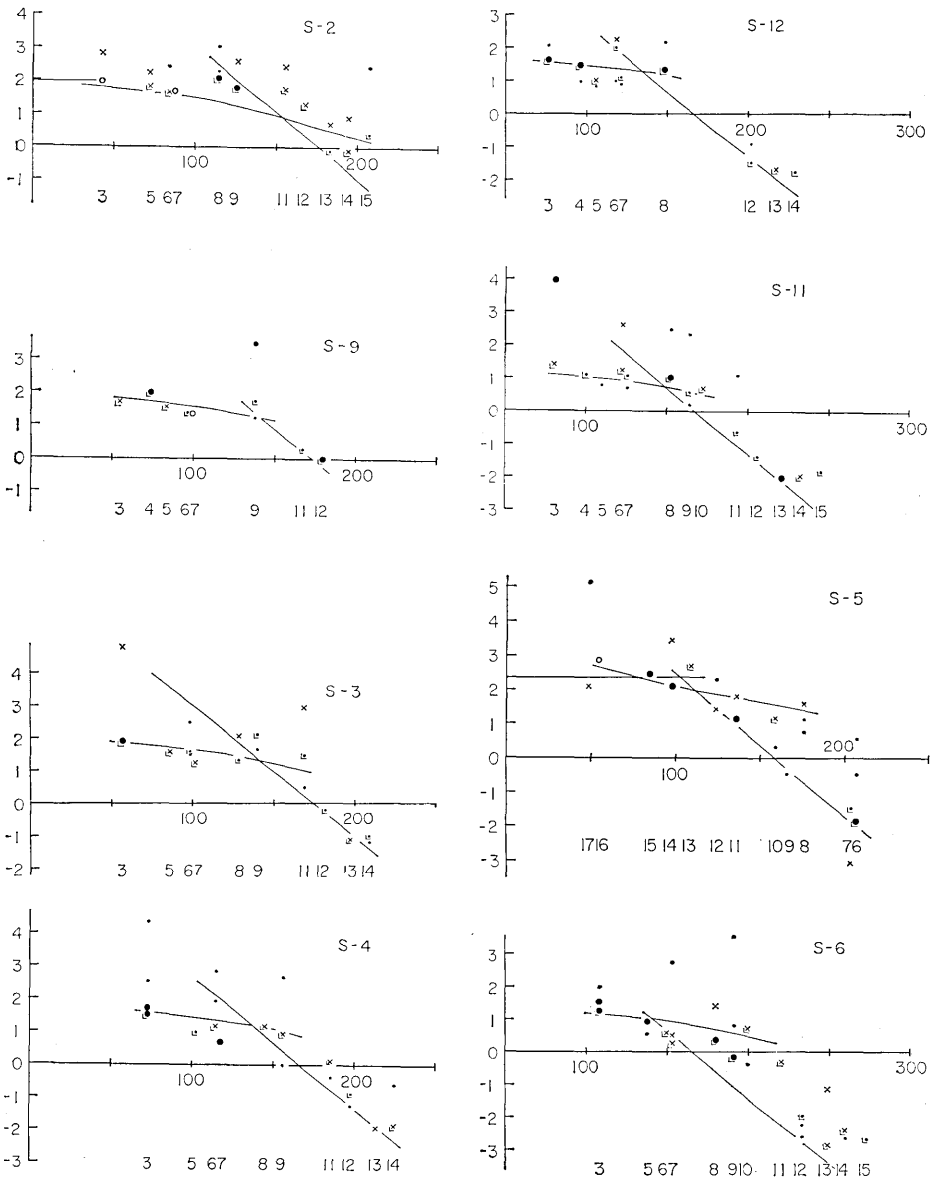

Fig. 3.
large closed circle: class B reading
cross mark : class C reading
small closed circle: class D reading
The plot with ⌊ means that although the signals can be identified at this time with certainty, the initial might be earlier than the reading. The numbers beneath each plot give the station numbers in Table 2 of Part 1. The travel time curves derived from the model of Fig. 10 are inserted.

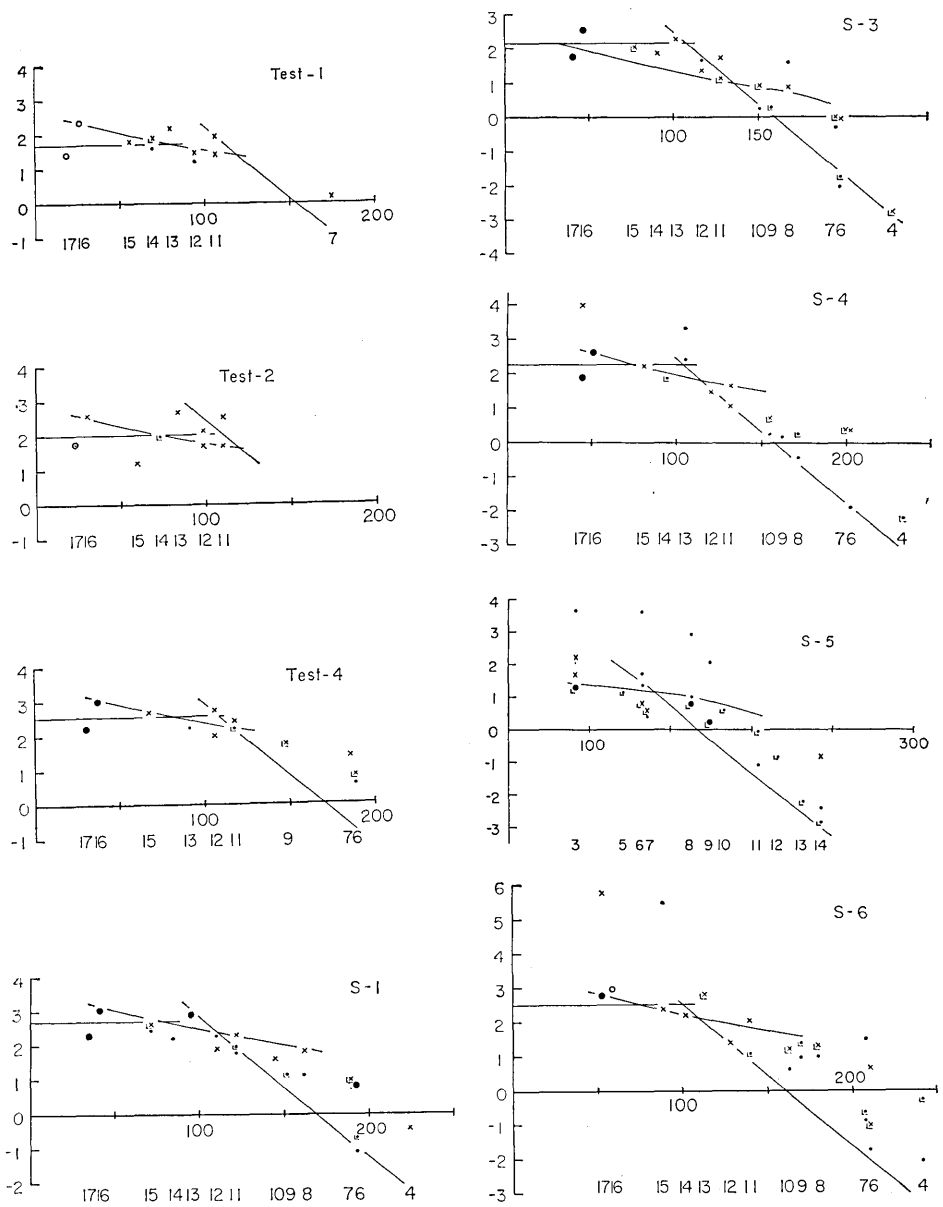

Fig. 4. Reduced travel time plot for each shot in the Off Oga Peninsula explosions.
abscissa : epicentral distance Δ in km.
ordinate : reduced travel time (T-Δ/6) in sec.
⊙ : class A reading
large closed circle: class B reading

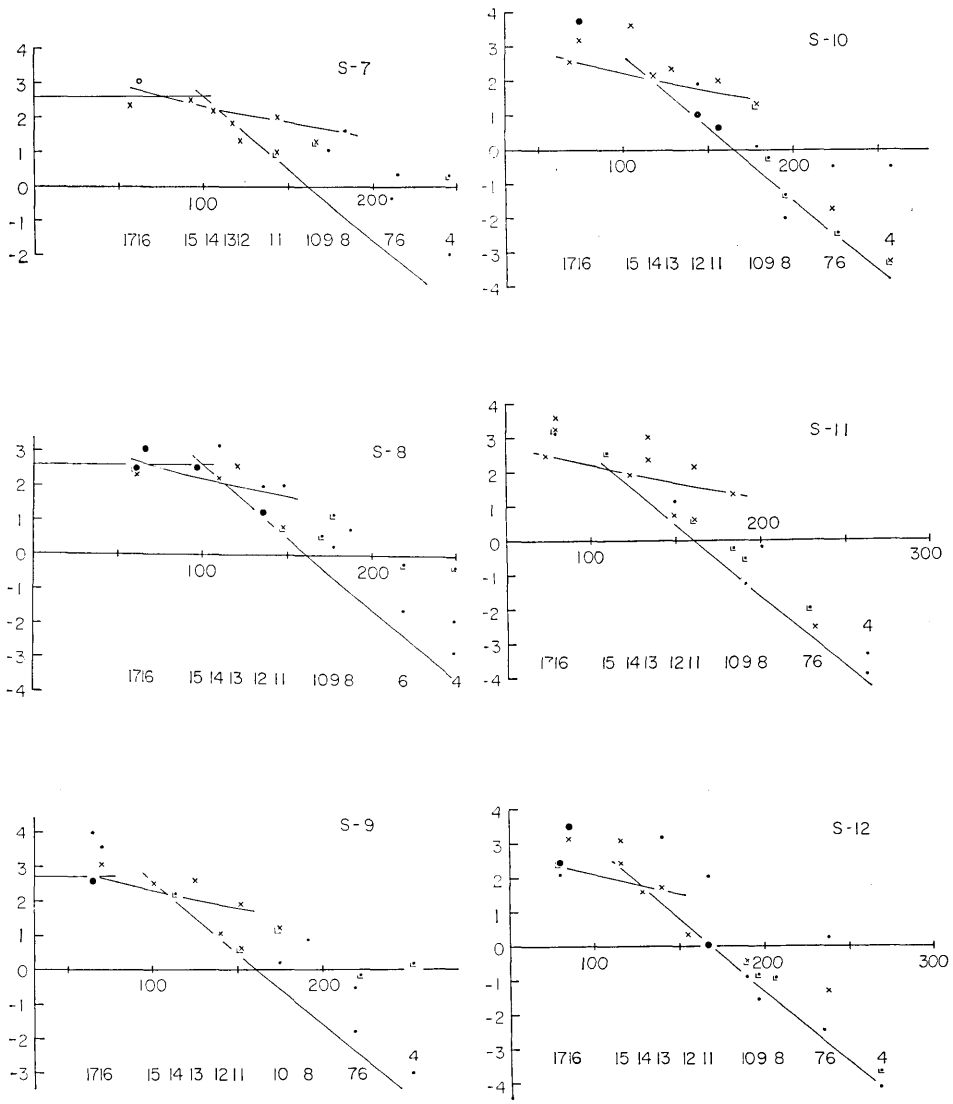

Fig. 4.

cross mark : class C reading

small closed circle: class D reading

The plot with ⌊ means that although the signals can be identified at this time with certainty, the initial might be earlier than the reading. The numbers beneath each plot give the stations numbers in Table 4 of Part 1. The travel time curves derived from the model of Fig. 10 are inserted.

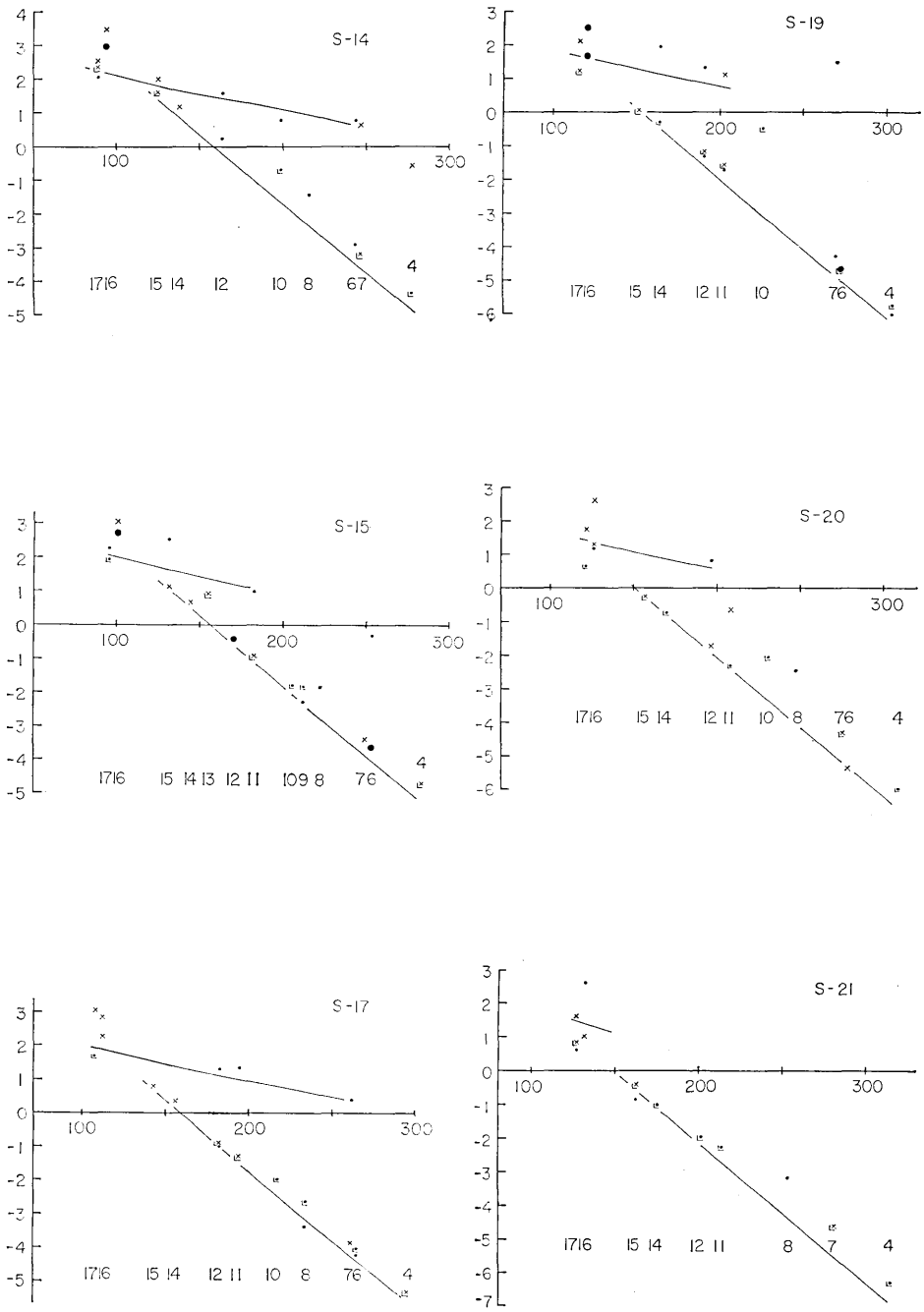

Fig. 4.

The flow diagram of the analytical procedures is given in Fig. 1. According to the flow diagram, the final results in each stage will be described.

In this paper, for simplicity's sake, the following abbreviations are used:

travel time plot for each shot in the Off Kesennuma explosions: K-shot travel time plot,

travel time plot for each shot in the Off Oga Peninsula explosions: O-shot travel time plot,

travel time plot for each station in the Off Kesennuma explosions: K-station travel time plot,

travel time plot for each station in the Off Oga Peninsula explosions: O-station travel time plot,

travel time plot for the receiving vessel: RV. travel time plot,

travel time plot for the Tutihata explosion: T. travel time plot,

shot No. 2: S2,

test shot No. 31: T31.

Also for convenience' sake the layer with P wave velocity of about 6 km/s is called the granitic layer and the layer above this one, the surface layer on land and the sedimentary layer at the sea bottom. Furthermore, the layer with P wave velocity of about 6.6 km/s is called the basaltic layer and the lower interface of this layer, the Moho discontinuity.

Stage A Velocity determination of the granitic layer

In Fig. 2, the RV. travel time plot is given. It was assumed for the topographic correction that the change in thickness of the topmost sedimentary layer with velocity of 2 km/s causes the deviation of the sea bottom from the adopted base lines. As seen from the figure, the apparent velocity of about 6.1 km/s is obtained. The true velocity is calculated to be 5.9 km/s by taking account of the dip of the base line.

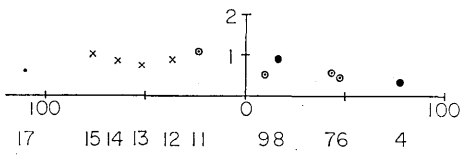

Fig. 5. Reduced travel time plot in the Tutihata explosion.
abscissa: epicentral distance Δ in km.
ordinate: reduced travel time (T-Δ/6) in sec.
◉ : class A reading
large closed circle: class B reading
cross mark : class C reading
small closed circle: class D reading
The numbers beneath each plot give the station numbers in Table 4 of Part 1.

The K-shot, the O-shot and

the T. travel time plots are given in Figs. 3, 4 and 5 respectively. From the K-shot travel time plots, the line with velocity of about 6.0 km/s can be fitted to the observed data. While from the K-station travel time plots obtained in Stage C (Fig. 9) this value of velocity is ascertained. In the T. travel time plot the velocity of 6.0-6.1 km/s was inferred reasonably from some trials although the effect of the surface layer seems to be large. However, it is very difficult to obtain the velocity of the granitic layer from the O-shot travel time plots as seen from Fig. 4. From these circumstances, the velocity of the granitic layer is assumed to be 6.0 km/s and applied to the whole area concerned. This assumption is supported by the fact that in almost all explosion seismic experiments in Japan the value 6.0-6.1 km/s is obtained for the granitic layer.

Stage B Determination of the surface layer and the sedimentary layer

For the velocity of the topmost sediment the value of 2.0 km/s can be assumed since the value close to this is often found in the deep sea seismic experiments[3]. By first arrivals from T27 through T31, the velocity 5.0 km/s is determined in the RV. travel time plot. In the range larger than the distance of T32, the velocity of the granitic layer is obtained. The velocities, 5.0 and 6.0 km/s are very close to those obtained by the deep sea seismic experiments conducted in this vicinity[4]. By assuming horizontal layering, the crustal structure obtained is such that water, the 2.0 km/s layer and the 5.0 km/s layer are 1.5 km, 2.0 km and 2.5 km in thickness respectively. Also in Fig. 2, observed data of granitic layer from shots closer to the coast than T39 or S5 show fairly large deviations from the 6.0 km/s line in spite of clear onsets. These deviations might be attributable to change in thickness of sediments at the shot points or under the receiving vessel. Although the positions of S11 and S12 are between those of S4 and S5, the difference of residuals between the data of the former and of the latter is about 0.5 sec. This is probably due to the change in thickness of sediment under the receiving vessel, the drift of which was fairly large as shown in Fig. 1 of Part 1. However, at present no data are available to examine this kind of effect in more detail.

3) R. E. HOUTZ and J. I. EWING, *Bull. Seism. Soc. Amer.*, **54** (1964), 867.

4) W. J. LUDWIG, J. I. EWING, M. EWING, S. MURAUCHI, N. DEN, S. ASANO, H. HOTTA, M. HAYAKAWA, T. ASANUMA, K. ICHIKAWA, and I. NOGUCHI, *J. Geophys. Res.*, **71** (1966), 2121.

In the K-shot travel time plots (Fig. 3), the line of 6.0 km/s gives the intercept time, which relates to the thickness of sediments at station and shot concerned. Assuming that the surface layer with velocity of 5.5 km/s exists on land above the granitic layer, being 3.0 km in thickness, the contribution from the sedimentary layer at sea bottom to the intercept time can be deduced. For this purpose the data of land stations from the shots closer to the coast than S9 and those of the receiving vessel from S5 and S6 are available as mentioned above. Since the velocity of 6.0 km/s could not be determined for shots S3, S4, S11, S12, the intercept time of the sedimentary layer was obtained by means of interpolation (Fig. 6a). The above intercept time contribution

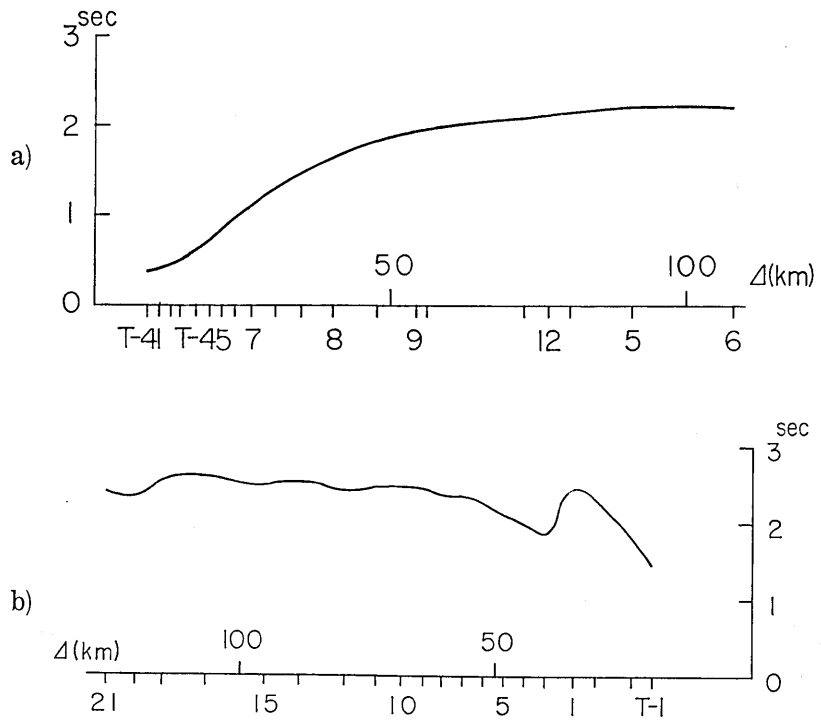

Fig. 6. Intercept times of the line of 6.0 km/s derived from the travel time plot for each shot. Numbers under the abscissa such as T-1, 5, 8 mean the shot numbers. For example, T-1 is test shot No. 1 and 5 is shot No. 5.

a) The Off Kesennuma explosions. The abscissa is the epicentral distance Δ from Station Karakuwa.

b) The Off Oga Peninsula explosions. The abscissa is the epicentral distance Δ from Station Monzen.

derived from shot points between T41 and S9 and from those of S5 and S6 is fairly reliable and the error is supposed to be less than 0.1-0.2 sec.

Next, in the O-shot travel time plots the 6.0 km/s line is hard to determine as mentioned in Stage A. This is because the observed data of Monzen are earlier by about 0.5 sec, and those of Kanpuzan, delayed by about 0.5 sec, from 6.0 km/s lines drawn tentatively although the seismograms of Monzen and Kanpuzan are quite good as shown in Fig. 6 of Part 1. An alternate interpretation is that the travel times of Monzen are relatively small by about 1.0 sec and the first arrivals of Kanpuzan belong to the line 6.6 km/s determined in Stage C. According to this interpretation, however, even at Monzen there exists an oceanic crust which is devoid of the granitic layer and it becomes difficult to connect this structure with that compatible with the data of the Off Kesennuma explosions. Also this oceanic crust would be against the results of an explosion seismic experiment in a profile between Monzen and Yahiko[5]. Since observed data of Matubara and Kayamori roughly fit to the 6.0 km/s line, this value was adopted for further interpretation. Up to S9, the 6.0 km/s lines were barely drawn, so that contributions of sedimentary layer to the intercept time could be estimated by means of procedures mentioned previously. For shots farther than S10 two models for sedimentary layers were considered since the line 6.0 km/s could not be drawn any longer. In the first model the sedimentary layers at S9 are extended up to S21 as they are. While in the second model, the total thickness of sedimentary layers at S21 is half of that at S9 and decreases monotonously between these two shots.

In Fig. 6a, b the values of intercept time contribution from the sedimentary layers are given.

Combining these values with the velocity and the ratio of thickness of layers obtained from the RV. travel time plot, the total thickness of sedimentary layers at each shot point was derived as shown in Fig. 10. Up to about 50 km off Kesennuma the sedimentary layers become thicker gradually up to several kilometers thick including water[6]. Off Oga

5) S. MURAUCHI, N. DEN, S. ASANO, H. HOTTA, T. ASANUMA, T. YOSHII, K. HAGIWARA, K. ICHIKAWA, S. IIZUKA, T. SATO and T. YASUI, *J. Phys. Earth*, in preparation.

6) According to the recent seismic profiling by S. MURAUCHI, H. HOTTA and T. ASANUMA in the shot point area off Kesennuma, the low velocity sediment with thickness around 1 km exists. This layer seems to be disturbed to a fairly large extent. However, this profiling has little effect on the general feature of deep structure in this paper.

Peninsula there is a similar tendency except that there is a little more fluctuation in layer thickness. The maximum thickness is also several kilometers.

In the T. travel time plot, the intercept time of the line 6.0 km/s for the eastern profile is about 0.5 sec and that for the western profile, about 1.0 sec. The difference is about 0.5 sec and the apparent velocity in the eastern profile is slightly larger than that in the western profile. For shallow structure, from these observations, it is possible to construct a model which has the surface layer of 5.5 km/s thinning towards the east. Observations near Tutihata shot point give the apparent velocity of about 3.0 km/s.

Stage C Reduction of travel times replacing the surface sedimentary layers by the granitic layer

The correction Δt to the travel time of waves propagating through the layer with velocity of v_i is given on the assumption of layered structure by

$$\Delta t = r_1/v_1 + r_2/v_2 + r_3/v_3 + \{(r_5 - r_7)/v_i\} \cdot (r_6/v_4)$$

where v_1 is the velocity of sea water, v_2 and v_3, that of sedimentary layers and v_4, that of the granitic layer (Fig. 7). The velocity and the ratio of thickness of sedimentary layers for the area off Kesennuma as well as off Oga Peninsula were assumed to be the same as those obtained from the RV. travel time plot in the Off Kesennuma explosions. As far as the 6.0 km/s line is fixed in the travel time plots, the error introduced by the above assumption is supposed to be small.

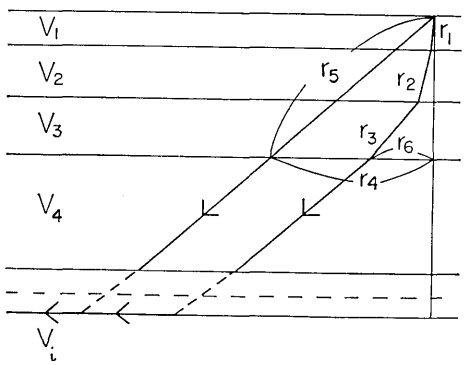

Fig. 7. Schematic illustration of seismic rays for reduction.

In Figs. 8 and 9, the K- and the O-station travel time plots obtained by replacing water and sedimentary layers by the granitic layer are given. These travel time plots are regarded as the reverse profiles of the K- or the O-shot travel time plots for layers deeper than the granitic layer. There remain some regional variations of surface structure on land as mentioned later.

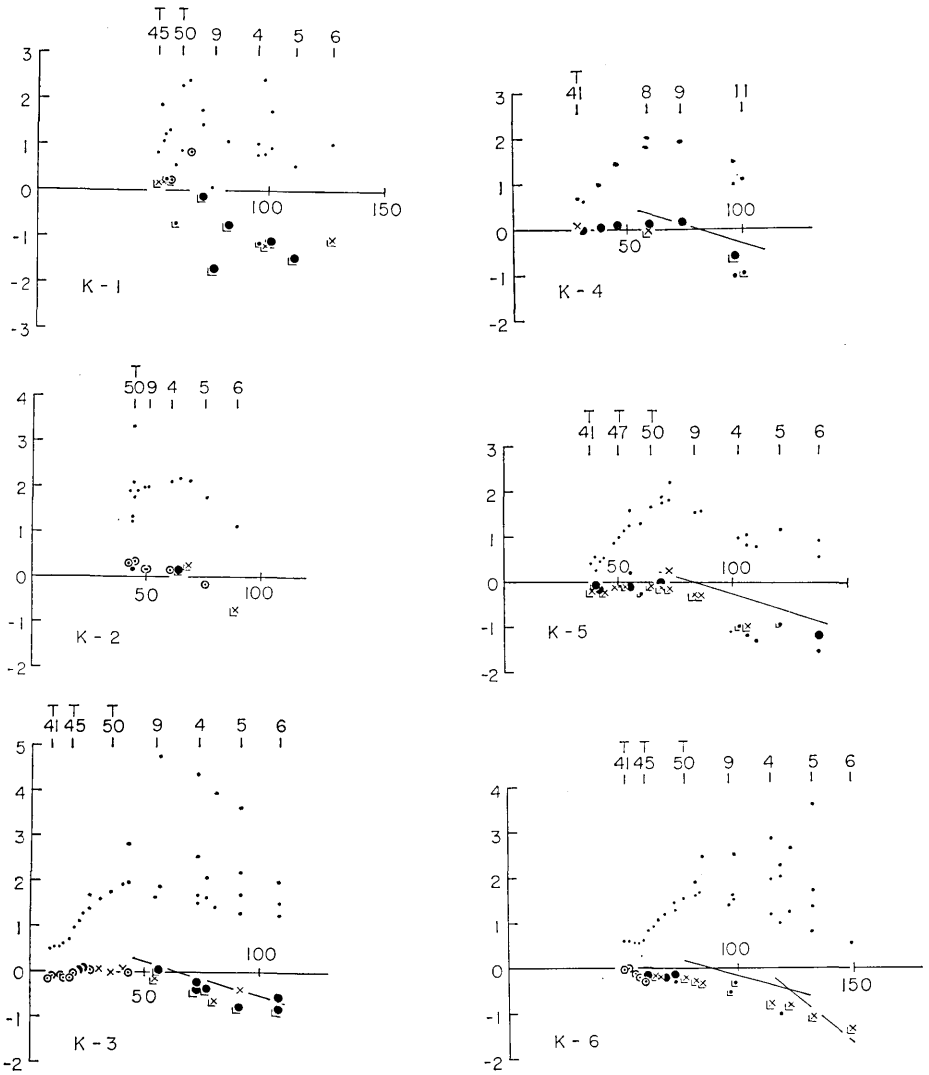

Fig. 8. Reduced travel time plot for each station in the Off Kesennuma explosions.
abscissa : epicentral distance Δ in km.
ordinate : reduced travel time (T-Δ/6) in sec.
⊙ : class A reading
large closed circle: class B reading
cross mark : class C reading
small closed circle: class D reading
The plot with ⌊ means that although the signals can be identified at this time with certainty, the initial might be earlier than the reading. The numbers above each plot give the shot numbers in Table 1 of Part 1. In these plots, the reduction replacing sea water, surface and sedimentary layers by the granitic layer are applied. The smallest closed circles are original plots. The travel time curves derived from the model of Fig. 10 are inserted.

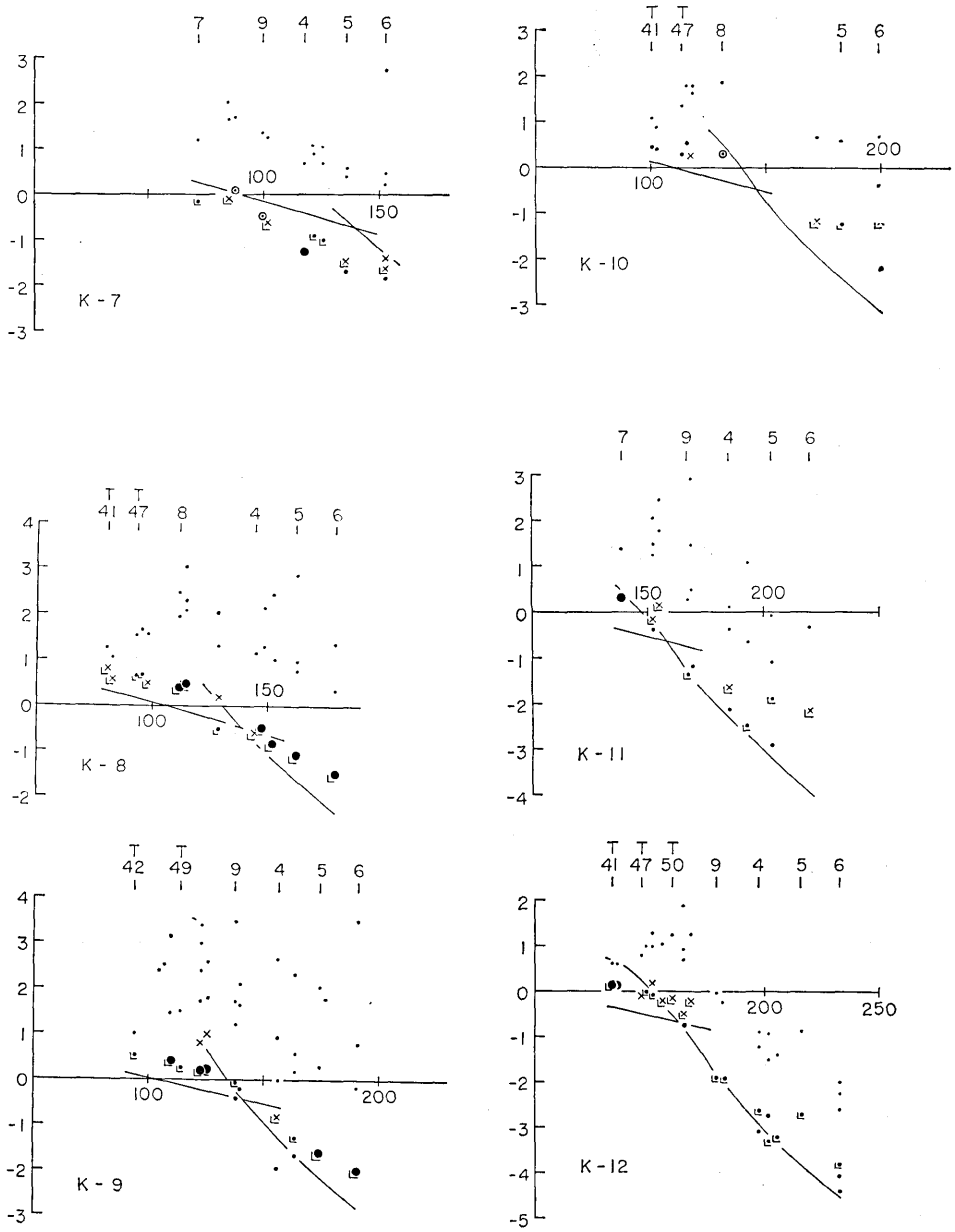

Fig. 8

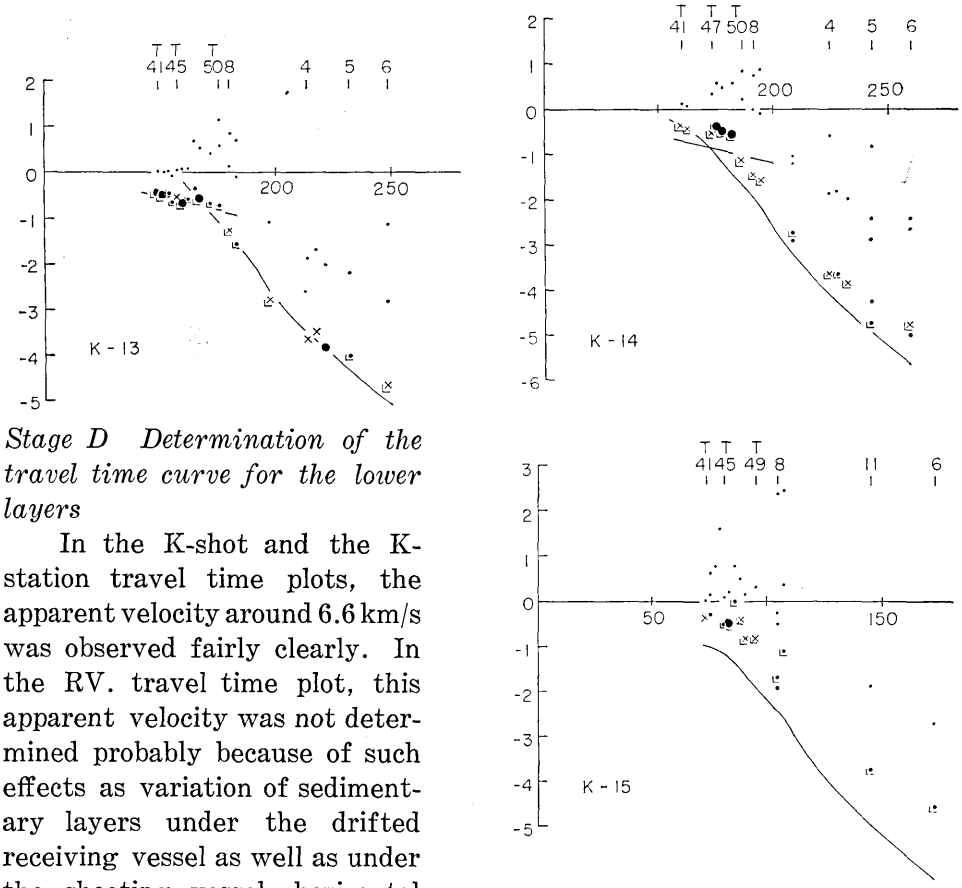

Fig. 8

Stage D Determination of the travel time curve for the lower layers

In the K-shot and the K-station travel time plots, the apparent velocity around 6.6 km/s was observed fairly clearly. In the RV. travel time plot, this apparent velocity was not determined probably because of such effects as variation of sedimentary layers under the drifted receiving vessel as well as under the shooting vessel, horizontal variations of sound velocity in water, etc.

In the Off Oga Peninsula explosions, it is not easy to determine the apparent velocity of the basaltic layer although the apparent velocity for some of the first arrivals give the value around 6.6 km/s. From the K-shot and the K-station travel time plots, the value of 6.6 km/s was tentatively assumed for the velocity of the basaltic layer throughout this profile.

As regards Pn velocity the O-shot and the O-station travel time plots give good determination. From almost all the O-shot travel time plots, the apparent velocity of about 8.0 km/s was determined fairly well. In the O-station travel time plots, however, the velocity greater than 8.0 km/s was obtained as a whole. Especially the apparent velocity for S9 through S21 is greater than 9 km/s. If the velocity and thickness

of sedimentary layers in the area of S9 through S21 are assumed to be the same as those in S8, the apparent velocity becomes about 9.4 km/s. Assuming the gradual decrease in thickness of sedimentary layers in the area from S8 to S21, the apparent velocity of 9.0 km/s is obtained.

Generally speaking, the determination of apparent velocity is not easy in the Off Kesennuma explosions, probably because of the complicated structure in the coastal area. From the travel time plots for stations or shots far from the coast which are supposed to be affected little by the complicated structure near the shore, the apparent velocity of about 8.0 km/s was determined. After some cyclic trials between Stages E and D, 6.6 km/s and 8.0 km/s were determined for the velocities of the basaltic layer and of Pn respectively.

From the T. travel time plot, the velocity of the layer deeper than the basaltic layer could not be determined.

Stage E Determination of crustal structure

From the apparent velocity, the cross-over distance or the intercept time determined through Stage D, the crustal structure of the first approximation can be derived. Starting from the model of first approximation, the final model of crustal structure in Fig. 10 was derived after some cyclic trials based on the flow diagram of Fig. 1. Off Oga Peninsula the interfaces between layers are shown by broken lines since no observed data on the sedimentary layers are available.

The main features of this model are as follows:

i) *The interface between the granitic and the basaltic layers*

On land the depth of this interface is about 15 km and this interface is fairly flat. In the vicinity of the coast, the granitic layer gradually becomes thin toward the Pacific Ocean and the Sea of Japan. In the borderland of the Pacific side the interface is about 8 km in depth, and this structure continues up to the area of S6. Taking water and sedimentary layers into account, the granitic layer is quite thin. While, in the borderland on the side of the Sea of Japan, the interface is about 10 km in depth and also seems to become quite thin or disappear farther than 50 km Off Oga peninsula.

ii) *The depth of the Moho discontinuity*

On land the depth of Moho discontinuity is about 30 km and fairly flat like the above interface. The crust, however, tapers near the coast toward the ocean and is about 20 km in thickness about 50 km off the coast of the Pacific Ocean. In this profile, on the side of the Pacific

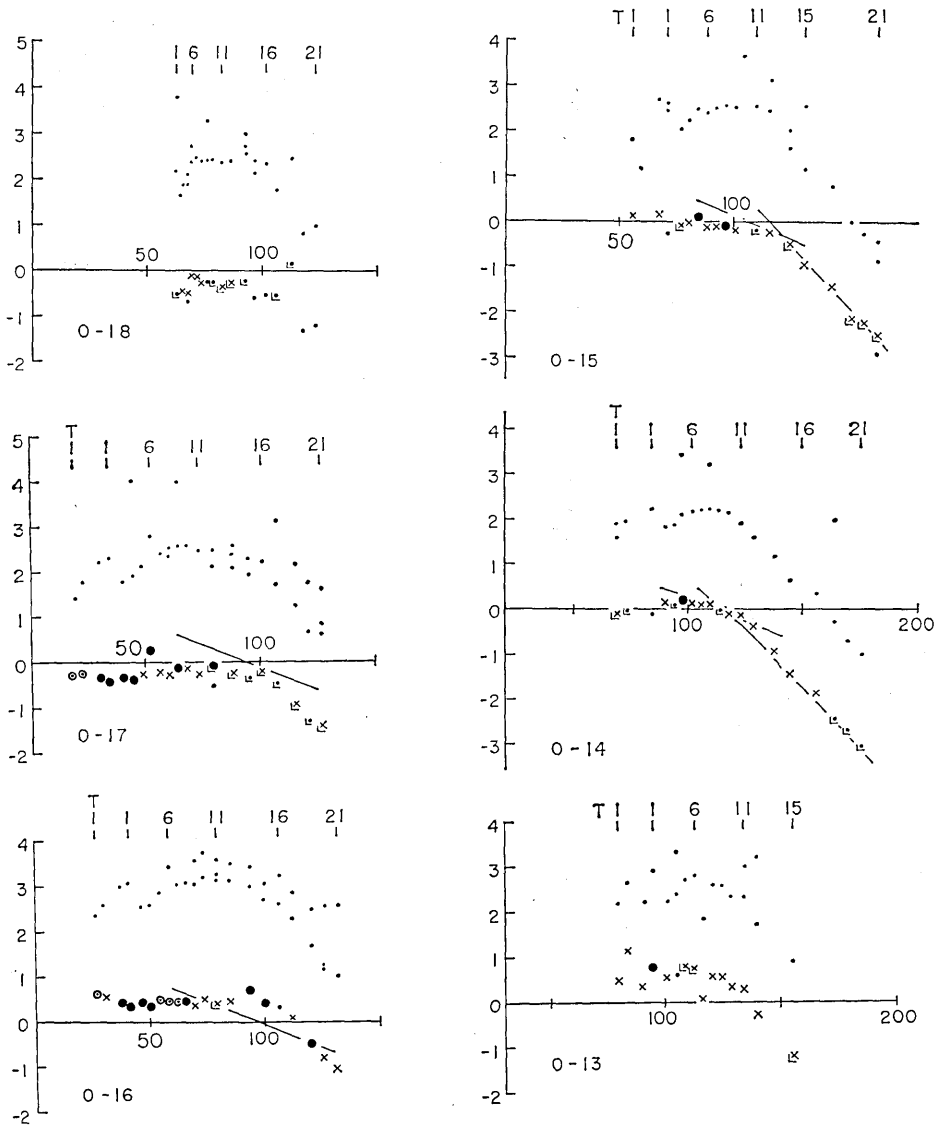

Fig. 9. Reduced travel time plot for each station in the Off Oga Peninsula explosions.
abscissa: epicentral distance Δ in km.
ordinate: reduced travel time (T-Δ/6) in sec.
⊙ : class A reading cross mark : class C reading
large closed circle: class B reading small closed circle: class D reading
The plot with ⌊ means that although the signals can be identified at this time with certainty, the initial might be earlier than the reading. The numbers above each plot give the shot numbers in Table 2 of Part 1. In these plots, the reduction replacing sea water, surface and sedimentary layers by the granitic layer are applied. The smallest closed circles are original plots. The travel time curves derived from the model of Fig. 10 are inserted.

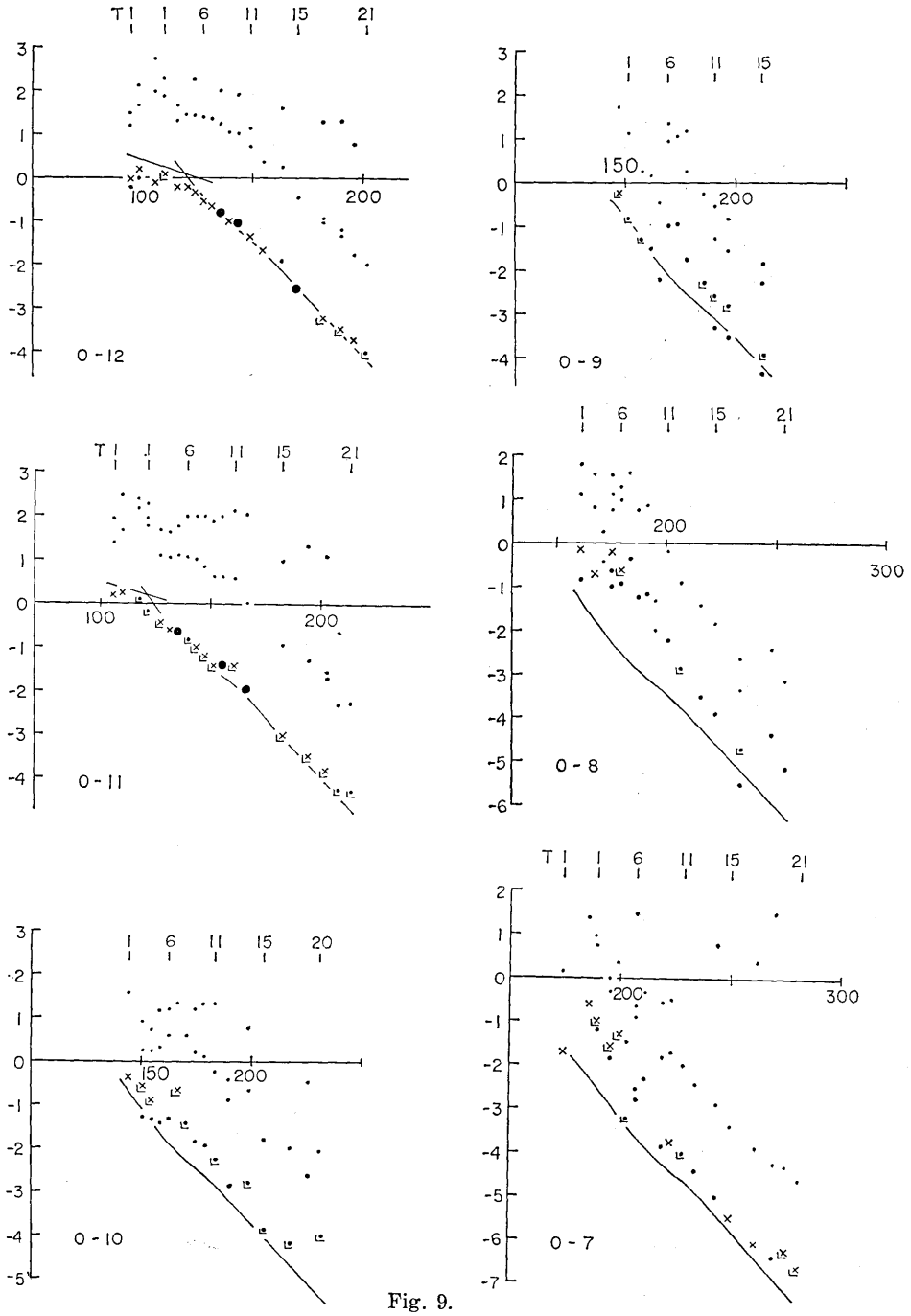

Fig. 9.

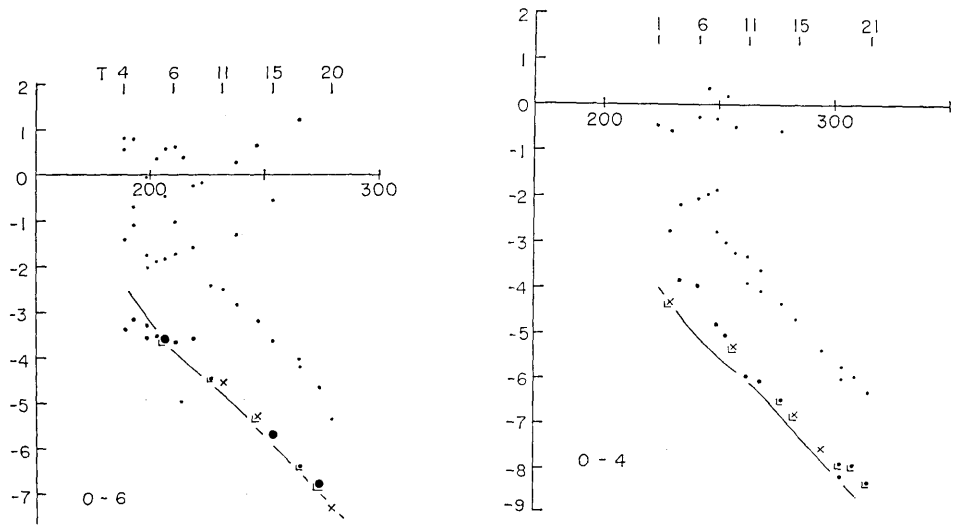

Fig. 9.

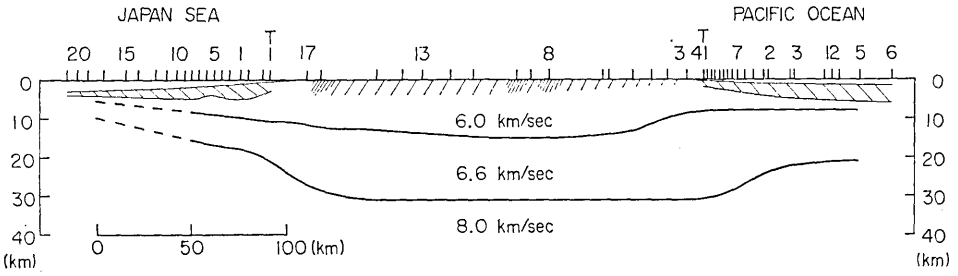

Fig. 10. Model of crustal structure along the profile. Numbers at sea mean shot numbers and those on land mean station numbers. Hatched parts designate surface or sedimentary layers. Thick hatched parts show that the existence of low velocity layers can be expected.

Ocean, the crustal structure becomes oceanic fairly rapidly as the distance from the Japanese island increases. While in the Sea of Japan, the crust is thinner near the coast than the Pacific side and tapers rapidly. In the area with water depth of 3000 m, about 100 km west of Oga Peninsula, the crustal structure is fairly oceanic. Therefore, as far as the cross section along the profile is concerned, the transition of crustal structure from the continental to the oceanic seems to occur in the vicinity of the Japanese island. This might give important data to study the development of the Japanese islands.

In Figs. 8 and 9, travel time curves calculated graphically from the

model of Fig. 10 are given. Generally speaking, the agreement between observed and calculated travel times is fairly good. However, some of the observations show unexpectedly large amounts of scatter. The fluctuation of travel times from station to station is possibly due to the variation of the surface geology. First, in the K-station travel time plots for Karakuwa through Mizusawa, the observed travel times of the basaltic layer are earlier than the calculated ones by about 0.5 sec. For stations farther than Iwasaki, the observed travel times of basaltic layer are delayed from the calculated ones except Miyatamata. The former discrepancy is considered to be due to a transitional complicated crustal structure in the concerned area. Furthermore, since the data of Miyatamata are of good quality and earlier than those at other stations, it was assumed that there could be no delay due to the surface layer at Miyatamata. The data of Matubara and Kayamori are delayed from the calculated travel times. Most of the first arrivals at Matubara were supposed to be missed because of high noise level, and the delay at Kayamori may be due to the surface layer. The data of the Tutihata explosion also support this interpretation.

In the K-shot travel time plots, the agreement between observed and calculated values for the granitic layer is fairly good. The calculated travel times of the basaltic layer up to S8 are less than the observed ones and those for shots farther than S9 have a tendency to be late. On the whole, the calculated values for 8.0 km/s layer are a little earlier than the observed.

Also there are some peculiar stations which give anomalous residuals. For example, residuals at Monzen are around -0.5 sec, and those of Kanpuzan, around $+0.5$ sec. The relative distance is less than 10 km and seismograms give clear first arrivals for both station. At present there is no reasonable explanation for this phenomenon.

Stations such as Iwasaki, Yuda (Yukawa, Tutihata) also give fairly large delays for the Off Kesennuma as well as the Off Oga Peninsula explosions. Taking data of the Tutihata explosion into account, there is a complicated surface structure in the central mountain area. In Fig. 10, the surface layer is shown by hatch although it is rather qualitative. The thick hatch shows that there should exist a low velocity surface layer.

Some of stations other than those mentioned above give large deviations. These deviations as well as systematic ones mentioned previously are caused by the following possibilities:

There might be a structure with faults or with horizontal inhomogeneity ; some of the initials might be missed because of their smallness; there might be complicated local surface structure around observation sites or shot points and so on.

Therefore, neglecting the above possibilities, the general trend of deep structure is looked for in this analysis. Detailed analysis to reduce deviations at each station is left for future studies.

In Figs. 8 and 9, the K-station travel time plots of Kamaisi and Enosima and the O-station travel time plot of Iwadate are included respectively. Since the station travel time plots of Kamaisi and Enosima, which are not on the profile, resemble the station travel time plot of Karakuwa and the station travel time plot of Iwadate is similar to that of Monzen, the model presented in Fig. 10 might be extended to farther north and farther south.

Furthermore, it is noted that the station travel time plots for Yuda and Yukawa, which are very close to Tutihata, lie on the extension of the travel time plot of the Tutihata explosion. This gives an additional support for the model, since the station travel time plot is equivalent to the travel time plot in the fictitious case of a shot at the real station and observation sites at the actual shot points.

3. Discussions

i) Through the analysis of Section 2, the velocities 6.0, 6.6, and 8.0 km/s are adopted for the granitic and the basaltic layers and the top of mantle respectively. If the velocities of layers are modified by 2%, the change of thickness is about 10% in the section with flat interfaces. Also if the thickness of each layer is varied by 1 km, the travel time might be affected by about 0.15 sec. Since the fluctuations of observed data are of the order of about 0.2 sec, general features of deep structure are acceptable.

As mentioned in Part 1, the data used were obtained at stations on land with shots at sea for the first time in Japan. Seismograms obtained are given in Figs. 4-6 of Part 1. In the figures the travel time curves derived from the model (Fig. 10 in this paper) are inserted. One of the differences in these seismograms from those of shots on land is the smallness of the first arrivals in comparison with the maximum amplitude. Therefore, some of the first arrivals may be missing. Also there is a possibility that the assumption of homogeneous layered structure

can not be applied for these complicated areas.

ii) Comparison with the previous results obtained by explosion seismic observations around this area

a. Previous results by the Research Group for Explosion Seismology

In this district the explosion seismic investigation was carried out by our Group for the first time in Japan[7]. The locations of profiles studied were a little different from the new profile. According to the former model, in the central mountains of this district the layer with velocity of about 6.1 km/s exists deeper than 10 km under the layer 5.8 km/s. This is unreasonable from the new data, but the old data can be explained satisfactorily through the new interpretation.

Furthermore the existence of the basaltic layer in Japan becomes more convincing as far as the layered structure is assumed. Also in this paper, the velocity of 8.0 km/s below the Moho discontinuity, which was first obtained in the western part of Honshu[8], was ascertained and gave reasonable travel times.

b. Results of deep sea seismic experiment

Off Sanriku area, an explosion seismic experiment at sea was conducted[9]. The surveyed area is about 1.5° north of the area in this paper. The receiving vessel of our experiment was south of and between Profile 6 and 7 of that experiment.

The crustal structure off Sanriku area has a fairly thick granitic layer. From our data, the granitic layer becomes fairly thin in the borderland. The investigation of this disagreement is left for future studies.

In the Sea of Japan, the profile parallel to Honshu between Monzen and Yahiko through Awasima was studied by Murauchi et al[10]. Although there is a general agreement, our granitic layer is a little thinner than their model.

4. Conclusions

The first fixed array-moving shot point experiments in northeastern Japan were conducted in 1965 and 1966 as a part of the Upper Mantle Project. The model of crustal structure was derived with the assumption

7) T. MATUZAWA, *Bull. Earthq. Res. Inst.*, 37 (1959), 123.

8) M. HASHIZUME, O. KAWAMOTO, S. ASANO, I. MURAMATU, T. ASADA,, I. TAMAKI, and S. MURAUCHI, *Bull. Earthq. Res. Inst.*, **44** (1966), 109.

9) W. J. LUDWIG et al., *loc. cit.*, 4).

10) S. MURAUCHI et al., *loc. cit.*, 5).

of homogeneous layered structure. The velocities 6.0, 6.6, and 8.0 km/s were reasonably determined for the granitic and the basaltic layers and for the top of the mantle respectively. On land the interfaces are fairly flat and the crust is about 30 km in thickness. The crust tapers near the shore toward the ocean on the east and the west side. The transition of the continental crust to the oceanic seems to occur in the vicinity of the Japanese island in this cross section.

Acknowledgement

We wish to express our thanks to the members of the Research Group for Explosion Seismology for their fruitful discussions and advices. Our thanks are also due to Misses S. Sugimoto, K. Fujii and E. Iwata for their help in preparing tables and figures.

---

26. 爆破地震動観測による東北日本を横断する測線上の地殻構造
第 2 部　地殻構造

京都大学防災研究所　橋爪道郎
京都大学防災研究所　尾池和夫
東京大学地震研究所　浅野周三
東北大学理学部　浜口博之
東京大学地震研究所　岡田惇
国立科学博物館　村内必典
東京大学地震研究所　嶋悦三
秋田大学教育学部　野越三雄

Part 1 に提出された我国初の fixed array-moving shot point 法による 1965 年 3 月の宮城県気仙沼沖及び 1966 年 3 月の秋田県男鹿半島沖爆破及び 1966 年 3 月中点爆破として行なった岩手県土畑鉱山における爆破の観測資料を第 1 図に示される手続によって解析した. homogeneous layered structure の仮定, 0.2 秒程度の走時のばらつきを認め, すべての資料を全体として合わせるようにして第 11 図に示されるような構造のモデルを求めた. 速度は花崗岩層では 6.0 km/s, 玄武岩層では 6.6 km/s, Pn は 8.0 km/s なる値を求め全地域一様であるとした. 中央山岳地域では花崗岩層, 玄武岩層とも約 15 km, 地殻の厚さはほぼ 30 km である. この地殻は陸地では割合一様な厚さであるが海岸付近から太平洋, 日本海に向って薄くなり海洋化は割合島の近くで起っているようである. 堆積層は, かなり厚く数 km あると推定された.